Carcinogenesis vol.32 no.6 pp.897–903, 2011
doi:10.1093/carcin/bgr049
Advance Access publication March 17, 2011

Suppressed liver tumorigenesis in fat-1 mice with elevated omega-3 fatty acids is associated with increased omega-3 derived lipid mediators and reduced TNF-α

Karsten H.Weylandt[1,2,*,†], Lena F.Krause[1,2,†], Beate Gomolka[2], Cheng-Ying Chiu[2], Süleyman Bilal[1,2], Anja Nadolny[1,2], Simon F.Waechter[1,2], Andreas Fischer[2], Michael Rothe[3] and Jing X.Kang[1]

[1]Laboratory for Lipid Medicine and Technology, Massachusetts General Hospital and Harvard Medical School, Boston, MA 02114, USA, [2]Department of Hepatology and Gastroenterology, Charité University Medicine, Rudolf-Virchow-Hospital, 13353 Berlin, Germany and [3]Lipidomix GmbH, 13125 Berlin, Germany

*To whom correspondence should be addressed. Laboratory for Lipid Medicine and Technology, Massachusetts General Hospital, 149, 13th Street, Room 4433, Charlestown, MA 02129, USA. Tel: +617 291 4073; Fax: +1 617 726 6144;
Email: karsten.weylandt@charite.de
Correspondence may also be addressed to Jing X.Kang. Tel: +617 726 8509; Fax: +1 617 726 6144; Email: jxkang@partners.org

Liver tumors, particularly hepatocellular carcinoma (HCC), are a major cause of morbidity and mortality worldwide. The development of HCC is mostly associated with chronic inflammatory liver disease of various etiologies. Previous studies have shown that omega-3 (n-3) polyunsaturated fatty acids (PUFAs) dampen inflammation in the liver and decrease formation of tumor necrosis factor (TNF)-α.

In this study, we used the fat-1 transgenic mouse model, which endogenously forms n-3 PUFA from n-6 PUFA to determine the effect of an increased n-3 PUFA tissue status on tumor formation in the diethylnitrosamine (DEN)-induced liver tumor model.

Our results showed a decrease in tumor formation, in terms of size and number, in fat-1 mice compared with wild-type littermates. Plasma TNF-α levels and liver cyclooxygenase-2 expression were markedly lower in fat-1 mice. Furthermore, there was a decreased fibrotic activity in the livers of fat-1 mice. Lipidomics analyses of lipid mediators revealed significantly increased levels of the n-3 PUFA-derived 18-hydroxyeicosapentaenoic acid (18-HEPE) and 17-hydroxydocosahexaenoic acid (17-HDHA) in the livers of fat-1 animals treated with DEN. *In vitro* experiments showed that 18-HEPE and 17-HDHA could effectively suppress lipopolysacharide-triggered TNF-α formation in a murine macrophage cell line.

The results of this study provide evidence that an increased tissue status of n-3 PUFA suppresses liver tumorigenesis, probably through inhibiting liver inflammation. The findings also point to a potential anticancer role for the n-3 PUFA-derived lipid mediators 18-HEPE and 17-HDHA, which can downregulate the important proinflammatory and proproliferative factor TNF-α.

Introduction

Hepatocellular carcinoma (HCC) is one of the most common cancers worldwide and a leading cause of cancer mortality. HCC primarily occurs in chronically inflamed liver tissue and in the context of cirrhosis (1). Thus, treatment of chronic inflammatory liver diseases is an approach to prevention of HCC. Treatment of this tumor entity is mainly limited to surgical or local-ablative procedures (2). However, prognosis is poor, and most patients eventually succumb to the disease. Experimental studies have established a link between inflammation and hepatocellular carcinogenesis and have found an important role for tumor necrosis factor (TNF)-α in tumor development (3–6). TNF-α promotes liver cell proliferation in the context of chronic inflammation, leading to enhanced tumorigenesis in the liver.

Polyunsaturated fatty acids (PUFAs) such as the n-6 PUFA arachidonic acid (AA 20:4) and the n-3 PUFAs eicosapentaenoic acid (EPA, C22:5) and docosahexaenoic acid (DHA, C22:6) play an important role in inflammation and proliferation as precursors of highly potent pro- and anti-inflammatory mediators (7). Several studies have implicated n-3 PUFA in the dampening of inflammation in the liver by a TNF-α-dependent mechanism (8,9). In a previous study in fat-1 mice with a balanced n-6/n-3 PUFA tissue content, lower inflammatory TNF-α levels and less severe tissue damage following D-Gal/lipopolysacharide (LPS)-triggered acute hepatitis were observed as compared with wild-type (wt) mice (8). Another study demonstrated that DHA supplementation led to increased formation of DHA-derived lipid mediators such as 17-hydroxydocosahexaenoic acid (17-HDHA) and protectin D1 (PD1), which were able to protect the liver from CCL_4-induced necroinflammatory damage (9). This study also showed that the protective effect was associated with decreased hepatic cyclooxygenase (COX)-2 expression and that 17-HDHA can suppress TNF-α secretion from cultured murine macrophages.

Recent studies have analyzed lipidomic aspects in the context of non-alcoholic steatohepatitis (NASH) pathology (10,11), demonstrating an increase in the ratio of n-6 to n-3 PUFA in NASH liver tissue as well as in the plasma levels of the AA metabolites 5-HETE, 8-HETE and 15-HETE in the progression from normal to NASH. These data indicate that the liver is critical not only for lipoprotein and triglyceride metabolism but also for the conversion of essential PUFAs to bioactive lipid mediators, due to the expression of COX, lipoxygenase and cytochrome P450 enzymes. The n-6/n-3 PUFA ratio in liver tissue probably determines the lipid mediator profile generated and could thus be an important factor in the development of liver disease.

Fat-1 mice can endogenously synthesize n-3 PUFA from n-6 PUFA without using dietary supplementation (12), thereby eliminating potential confounding factors of diet (13). These mice were recently used in a genetic hepatoma model in mice containing mutations in c-myc and transforming growth factor-alpha (14), as well as in an inoculation liver tumor model (15). Both models demonstrated significant antitumor activity in the fat-1 mice. However, both studies focused primarily on protein analysis, notably demonstrating lower nuclear factor-kappaB and COX-2 expression in the fat-1 livers, respectively. Analysis of n-3 PUFA lipid metabolites was not performed so far.

We therefore decided to investigate the influence of an increased tissue status of n-3 PUFA and decreased n-6/n-3 PUFA ratio on chemically induced liver tumorigenesis as well as on lipid mediator formation in the fat-1 transgenic mouse model. A chemical carcinogen, diethylnitrosamine (DEN), was used to induce liver tumors. DEN is metabolized into an alkylating agent that induces DNA damage and mutations as well as hepatocyte death, leading to subsequent proliferation and regeneration dependent on cytokines (4).

The results presented here show that DEN-induced liver tumorigenesis was suppressed in fat-1 mice. This was accompanied by significantly increased levels of the n-3 PUFA metabolites 18-hydroxyeicosapentaenoic acid (18-HEPE) and 17-HDHA in liver tissue and decreased plasma levels of TNF-α in fat-1 mice compared with DEN-treated wt mice. In addition, both 18-HEPE and 17-HDHA were found to inhibit TNF-α secretion in response to LPS stimulation in

Abbreviations: AA, arachidonic acid; COX, cyclooxygenase; DEN, diethylnitrosamine; DHA, docosahexaenoic acid; EPA, eicosapentaenoic acid; HCC, hepatocellular carcinoma; 17-HDHA, 17-hydroxydocosahexaenoic acid; 18-HEPE, 18-hydroxyeicosapentaenoic acid; HGF, hepatocyte growth factor; IL, interleukin; LPS, lipopolysacharide; mRNA, messenger RNA; NASH, non-alcoholic steatohepatitis; PUFA, polyunsaturated fatty acid; SMA, smooth muscle actin; TNF, tumor necrosis factor; wt, wild-type.

[†]These authors contributed equally to this work.

© The Author 2011. Published by Oxford University Press. All rights reserved. For Permissions, please email: journals.permissions@oup.com

Downloaded from https://academic.oup.com/carcin/article/32/6/897/2463601 by guest on 20 August 2022

a murine macrophage cell line, supporting a protective effect of the n-3 PUFA via these bioactive metabolites.

Materials and methods

Animals

Transgenic fat-1 C57BL/6 mice were generated as described previously (12). Only heterozygous male mice were used in this study. Mice were fed with an identical diet rich in n-6 PUFA and low in n-3 PUFA (10% safflower oil). Mice were phenotyped according to the n-6/n-3 PUFA ratio in their tails determined by gas chromatography. All animals received care according to the institutional guidelines and experiments were approved by the Massachusetts General Hospital Subcommittee on Research Animal Care. For the experiments, $n = 6$ wt mice and $n = 9$ fat-1 mice were used.

Tumor induction and macroscopic tumor evaluation

Fifteen-day-old mice were injected intraperitoneally with 5 mg/kg DEN (Sigma-Aldrich, St. Louis, MO). After 8 months, mice were killed and livers and blood were removed for further analysis. Externally visible liver tumors were counted and measured by stereomicroscopy immediately after killing the animals.

Microscopic tissue evaluation

The median lobe of the liver was fixed in 4% formaldehyde overnight, dehydrated and embedded in paraffin. Sections of 5 μm were stained with hematoxylin and eosin, trichrome and reticulin stains, respectively, for analysis of histopathological changes by an experienced pathologist in a blinded fashion (16,17), using the following criteria: Necrosis (0 = absent, 1 = spotty necrosis, one or few necrotic hepatocytes, 2 = multifocal necrosis, 3 = bridging necrosis, 4 = confluent necrosis); fibrosis (0 = absent, normal lobular architecture, 1 = pericentral fibrosis, increased thickness of the central vein, 2 = central anastomoses, some fibrous septa connecting central veins, 3 = precirrhotic stage, fibrous septa with marked distortion of the liver lobules, 4 = cirrhosis, nodule regeneration surrounded by broad connective tissue septa); steatosis (percentage of tissue area, 0 = 0%, 1 = <33%, 2 = <66%, 3 = >66%). The inflammation score was then calculated by adding the scores for necrosis, fibrosis and steatosis. Liver tumors were evaluated by counting the number of neoplastic foci, size of detected tumors in millimeter, differentiation state (1 = well, 2 = moderately, 3 = poorly differentiated) and lymphovascular invasion (0 = absent, 1 = present). The trichrome stains were also used to quantify connective tissue in the liver. For this, three different areas per slide were assessed and content of the blue connective tissue stain evaluated using ImageQuant Software.

Immunostaining

Liver tissue was fixed in 10% neutral-buffered formalin overnight, followed by automated processing and embedding in paraffin. F4/80 staining was performed on 3.5 μm deparaffinized tissue slides using a biotinylated anti-murine F4/80 antibody (eBioscience, San Diego, CA) at 1:100 dilution, for 1 h at room temperature. Slides were counterstained with hematoxylin. For α-smooth muscle actin (SMA) staining, the slides were exposed to a 1:25 diluted anti-α-SMA antibody (Thermo-Fischer Scientific, Waltham, MA) for 10 min at room temperature. After washing with phosphate-buffered saline, the primary anti-α-SMA antibody was detected using an Alexa fluor 594 antibody (Invitrogen, Carlsbad, CA). α-SMA-positive cells were counted in 3–5 high power fields per mouse by two different blinded observers, positive cells located in or near blood vessel walls were ignored, and the mean value of these counts was used for further analysis. Data are expressed as the number of α-SMA-positive cells per high power field. For visualization of liver cell nuclei, cells were costained with 4,6-diamine-2-phenylindole dihydrochloride (Sigma-Aldrich, St. Louis, MO), in an aqueous dilution of 1:10.000 for 2 min. For COX-2 determination, fresh-frozen sections were incubated overnight with an anti-murine COX-2 antibody (Cayman Chemical, Ann Arbor, MI), followed by staining with an horseradish peroxidase secondary antibody detected by diaminobenzidene substrate and counterstained with hematoxylin. Total-positive area per area of tissue was then analyzed using ImageQuant Software.

Lipid mediator analysis

Thirty milligrams ground and frozen liver tissue was mixed with methanol and internal standard (LTB_4-d_4) and hydrolyzed with 300 μl of 10 M sodium hydroxide for 30 min at 60°C. The solution was neutralized with 60% acetic acid and pH was adjusted to 6.0 with sodium acetate buffer. A solid phase extraction was performed with an anion exchange column (Bond Elute Certify II, Agilent, Santa Clara, CA) as described previously (18). For elution, an *n*-hexane:ethyl acetate extraction mixture 25:75 with 1% acetic acid was used. The eluate was evaporated on a heating block at 40°C under a stream of nitrogen to obtain a solid residue. Residues were then dissolved in 70 μl acetonitrile. An Agilent 1200 HPLC system and a solvent system consisting of acetonitrile/0.1% formic acid in water was used. The gradient elution was started with 15% acetonitrile, this was increased within 10 min up to 90% and held for 10 min. The high-performance liquid chromatography was coupled with an Agilent 6410 Triplequad mass spectrometer with electrospray ionization source. Analysis of lipid mediators was performed using multiple reaction monitoring in negative mode.

Gas chromatography

For PUFA analysis, liver or tail tissues frozen in liquid nitrogen were homogenized. An aliquot of tissue homogenate was mixed in a glass methylation tube with 1.5 ml hexane and 1.5 ml boron triflouride. The mixture was heated to 100°C for 1 h under nitrogen, cooled to room temperature and methyl esters extracted in the hexane phase following addition of 1 ml H_2O. The samples were centrifuged for 5 min and the upper hexane layer was removed and concentrated under nitrogen. Fatty acid methyl esters were analyzed by gas chromatography using a fully automated HP 6890 system equipped with a flame ionization detector as described previously (8). Peaks were identified by comparison with PUFA standards (Nu-Chek-Prep, Elysian, MN), and area and its percentage for each resolved peak was analyzed using a Perkin–Elmer M1 integrator.

Semiquantitative real-time polymerase chain reaction

Total RNA was isolated from liver tissue using Trizol reagent (Invitrogen, Carlsbad, CA) following the manufacturer's instructions. RNA concentrations and purity were determined spectrometrically by their absorbance at 260 nm in relation to the absorbance at 280 nm. Reverse transcription of messenger RNA (mRNA) was performed using random hexamer primers. Real-time polymerase chain reaction was carried out using EVA Green in an ABI PRISM 9000 Light Cycler following the manufacturer's protocol. The sequences of the primers used are interleukin (IL)-1β forward, gCAACTgTTCCTgAACTCAACT and IL-1β reverse ATCTTTTggggTCCgTCAACT; hepatocyte growth factor (HGF) forward ATgTgggggACCAAACTTCTg, HGF reverse ggATggCgACATgAAgCAg and hypoxanthin-guanin-phosphoribosyltransferase forward TTgCgCTCATCTTAggCTTT, hypoxanthin-guanin-phosphoribosyltransferase reverse CAggCCAgACTTTgTTggAT. Means were standardized to hypoxanthin-guanin-phosphoribosyltransferase values. Results are expressed as fold expression as compared with the wt animals.

Cell culture

Murine macrophage RAW 264.7 cells were cultured in Dulbecco's modified Eagle's medium supplemented with 10% fetal bovine serum, 100 U/ml penicillin and 100 U/ml streptomycin. For experiments, cells were plated in 24-well plates at a density of 5×10^5 cells per well and incubated overnight. All experiments were performed in a humidified atmosphere under 5% CO_2 at 37C.

RAW 264.7 cells were preincubated for 2 h with either 500 nM 17-HDHA or 500 nM 18-HEPE; controls were treated with equal volumes of vehicle solvent solution (ethanol). After preincubation, the medium was aspirated and cells were stimulated with 0.5 μg/ml *Escherichia coli* LPS in medium for 4 h. Supernatants were then taken and frozen at −80°C until TNF-α was assayed. TNF-α was measured in cell culture supernatants using an ELISA kit (eBioscience) following the manufacturer's protocol.

Serum analyses

Liver injury was examined by measuring the circulating transaminases (Biotron Diagnostics, Hemet, CA), alanine transaminase and aspartate transaminase. TNF-α was measured in serum samples using an ELISA (eBioscience, San Diego, CA) following the manufacturer's protocol.

Statistical analysis

Analysis was performed with Prism 3.02v Software (GraphPad) or REST 2009 (Qiagen) for real-time polymerase chain reaction. Comparison was made using the Student's *t*-test or as indicated. All values are presented as the mean ± standard error of the mean or as indicated. Statistical significance was set at $P < 0.05$.

Results

After postmortem removal of the livers, the tumors visible on the organ surface were counted and measured. There were significant macroscopically visible differences in the surface tumor load between the two groups of mice. Representative livers from wt and fat-1 mice are shown in Figure 1A and B. Quantitative analysis showed that the total number of surface tumors >3 mm was significantly lower in the fat-1 mice than in their wt littermates (Figure 1C). There was also a highly significant difference in the diameters of the

Downloaded from https://academic.oup.com/carcin/article/32/6/897/2463601 by guest on 20 August 2022

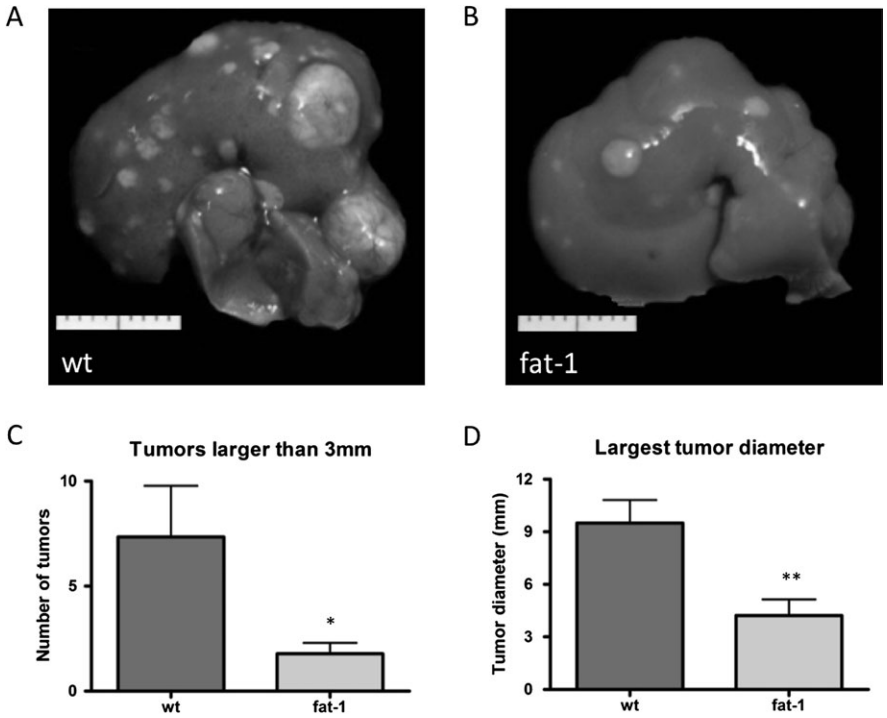

Fig. 1. Macroscopic evaluation of DEN-induced tumorigenesis. Representative postmortem photographs of livers from wt and fat-1 mice (**A** and **B**). Evaluation of surface-visible tumors >3 mm (**C**) and of the largest tumor diameters detectable (**D**) show a significant difference between wt and fat-1 mice ($^{**}P < 0.01$ and $^{*}P < 0.05$).

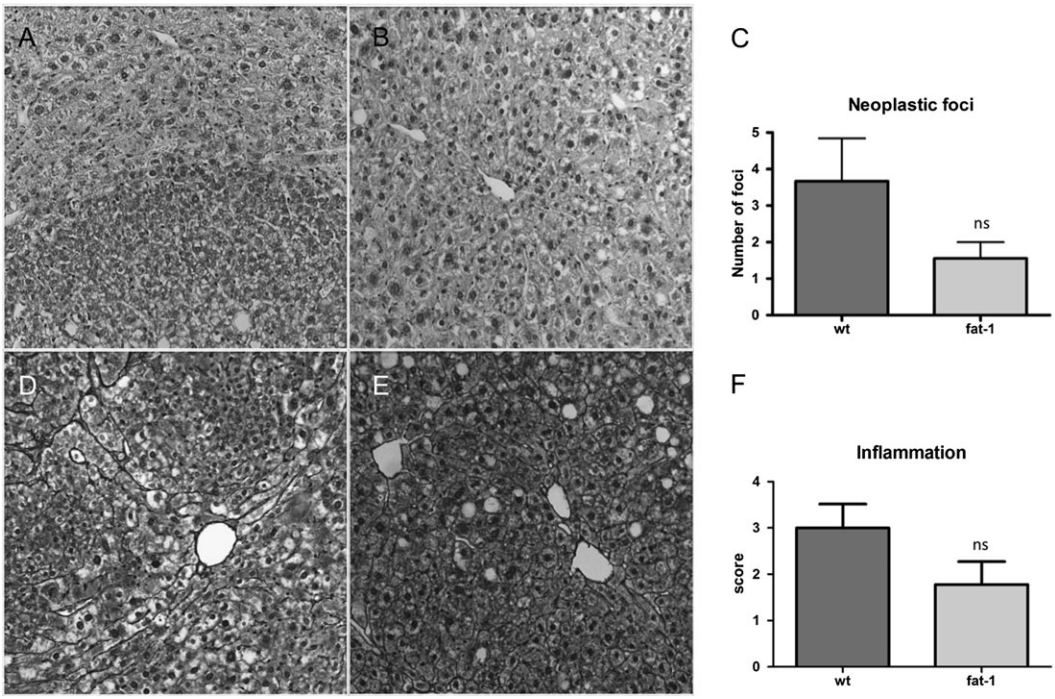

Fig. 2. Microscopic evaluation of representative hematoxylin and eosin (**A** and **B**) as well as reticulin (**D** and **E**) stains from the median liver lobe of DEN-treated wt (**A** and **D**) and fat-1 (**B** and **E**) animals. There were lower numbers of neoplastic foci in fat-1 mice (**C**), accompanied by a lower inflammation score in these mice (**F**), however, these differences were not significant (ns, not significant).

largest tumors discernible on the organ surface of each animal, with an average diameter of 9.5 mm in wt mice versus only 4.2 mm in the fat-1 mice (Figure 1D). The pathological evaluation of hematoxylin and eosin (Figure 2A and B) as well as reticulin (Figure 2D and E) stained slides from the median liver lobe showed a lower number of neoplastic foci in the DEN-treated fat-1 mice compared with the wt mice (Figure 2C), although that difference failed to reach statistical significance. The microscopically evaluated tumors in the wt group were of grade 2 (moderately differentiated) in three wt mice, with one wt mouse showing grade 3 (poorly differentiated) and only two wt

Downloaded from https://academic.oup.com/carcin/article/32/6/897/2463601 by guest on 20 August 2022

mice showing grade 1 (well differentiated) tumors. In contrast, there were no neoplastic lesions in the evaluated slides from two fat-1 mice and only one fat-1 mouse showed a grade 2 (moderately differentiated) lesion, whereas the remaining six fat-1 mice only had grade 1 (well differentiated) lesions. There was no lymphovascular invasion in either group of samples. Scoring of inflammatory changes indicated more inflammatory changes in the DEN-treated wt animals (Figure 2F).

To study the molecular basis for the observed anticancer effect in the fat-1 mice, we measured the levels of TNF-α and COX-2, which are known to play important roles in liver tumorigenesis and also performed a stain for macrophages in the liver tissue. While there were macrophages discernible in slides from four of five assayed wt mice (Figure 3A), no macrophages were discernible in the slides from the seven assayed fat-1 mice (Figure 3B). The plasma levels of TNF-α in the fat-1 mice with DEN-induced liver tumors were significantly lower than those in the wt mice (Figure 3C), which was accompanied by lower intrahepatic mRNA levels for IL-1β in the fat-1 mice (0.54-fold of wt, not significant at $P = 0.074$). The mRNA levels for the proproliferative HGF were lower in the fat-1 mouse group (0.77-fold of control $P = 0.05$). Immunhistochemical analysis of liver tissue demonstrated higher COX-2 expression in the livers of DEN-treated wt mice (Figure 3D) compared with fat-1 mice treated with DEN (Figure 3E and F), supporting the inflammation dampening effect observed in fat-1 mice.

In order to further examine the effect of the different n-3 PUFA tissue content on liver pathology, staining for α-SMA to visualize myofibroblasts and activated hepatic stellate cells (reflecting fibrogenic activity) in the livers of DEN-treated animals was performed and showed a significantly lower number of these cells in liver tissue from fat-1 mice (Figure 4A–C). In accordance with this finding, a significantly decreased connective tissue content in the fat-1 livers was documented in the trichrome stains (Figure 4D–F)

Furthermore, as indicators for the difference of liver cell damage between the two groups of animals, plasma alanine transaminase as well as aspartate transaminase levels were lower in the fat-1 mice as compared to their wt littermates, although the differences for aspartate transaminase were not significant (Figure 5A and B).

In order to quantify the major n-3 and n-6 PUFA and some of their metabolites, liver tissue from DEN-treated wt and fat-1 mice was analyzed using gas chromatography (Table I). Results of gas chromatography showed that the content of EPA and DHA was significantly different between the two groups, with higher levels in the fat-1 mice. There were lower levels of AA in the liver tissue of fat-1 animals as compared with the wt mice, but this difference was not statistically significant. Fat-1 mice had a ratio of AA/(DHA + EPA) of 1.97 ($n = 9$) compared with a ratio of 9.06 in wt mice ($n = 6$).

Next, we determined the profile of lipid mediators formed from these PUFA using liquid chromatography coupled tandem mass spectrometry. Analysis focused on the n-3 PUFA-derived monohydroxylated compounds 18-HEPE (derived from EPA) and 17-HDHA (derived from DHA) as well as the n-6 PUFA-derived 15-HETE (from AA). There was a highly significant difference in the liver tissue concentrations of 18-HEPE and 17-HDHA between fat-1 and wt mice. For 18-HEPE, tissue levels were 18.5 ± 3.1 ng/g in fat-1 mice versus non-detectable levels in wt mice (Figure 6A and C), for 17-HDHA, tissue levels in fat-1 mice reached 326.9 ± 38.3 ng/g versus 72.6 ± 23.9 ng/g in wt mice (Figure 6B and D). Compared with the baseline DHA levels in livers of fat-1 and wt animals, the 4.5-fold increase in 17-HDHA in fat-1 mice over wt mice compares with 4.2-fold higher tissue levels of DHA in fat-1 over wt mice. There were no significant differences in the 15-HETE levels between both groups of mice (data not shown).

In order to understand the physiological effects of 18-HEPE and 17-HDHA, these lipid metabolites were then tested directly for their ability to decrease TNF-α secretion from immune cells. These experiments were performed in the murine macrophage cell line RAW 264.7. Both 17-HDHA and 18-HEPE at a concentration of 0.5 μM were effective in decreasing LPS-induced TNF-α secretion ($n = 4$ independent experiments) (Figure 7). Although both metabolites were used in the same concentration (at 500 nM), 18-HEPE suppressed TNF-α more potently than 17-HDHA.

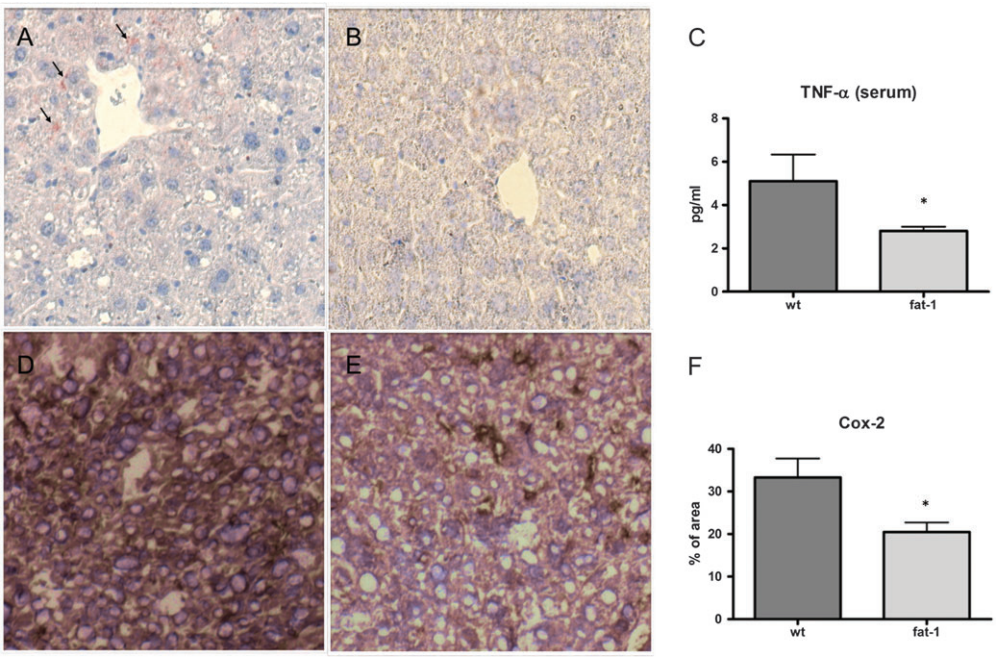

Fig. 3. Assessment of proinflammatory changes in wt and fat-1 mice with DEN-induced tumors. Analysis of F4/80-expression in DEN-treated animals demonstrated intraparenchymal macrophages (several are indicated by arrows) in most wt mice (**A**), while there were no F4/80-positive cells discernible in the fat-1 mouse samples assayed (**B**). Plasma TNF-α was decreased in DEN-treated fat-1 mice as compared with wt animals ($^*P < 0.05$) (**C**). Hepatic COX-2 expression in wt (**D**) and fat-1 (**E**) mice with DEN-induced liver tumors shows significantly lower protein expression in fat-1 mice (**F**) ($^*P < 0.05$).

Downloaded from https://academic.oup.com/carcin/article/32/6/897/2463601 by guest on 20 August 2022

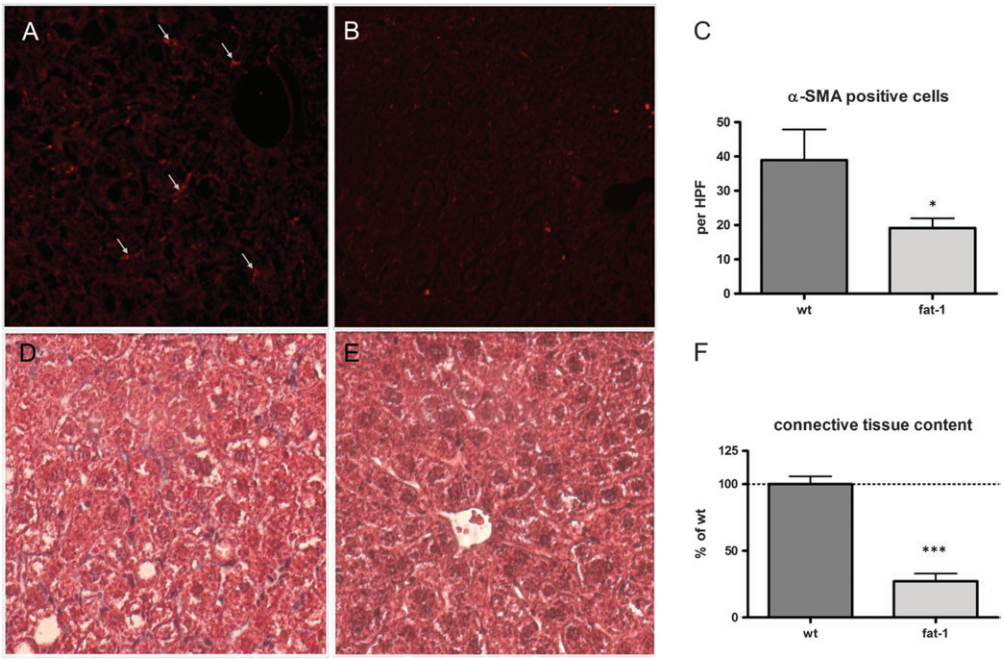

Fig. 4. Indications of decreased hepatic fibrogenesis in fat-1 mice. Wt mice (**A**) showed significantly more α-SMA-positive activated hepatic stellate cells and myofibroblasts (some indicated by arrows) than fat-1 mice (**B**) as quantified in the slides (**C**) ($^{*}P < 0.05$). Assessment in trichrome stains confirmed increased connective tissue in livers from wt mice (**D**) as compared with fat-1 mice (**E**), the quantity of blue connective tissue was compared between both groups (**F**) ($^{***}P < 0.001$).

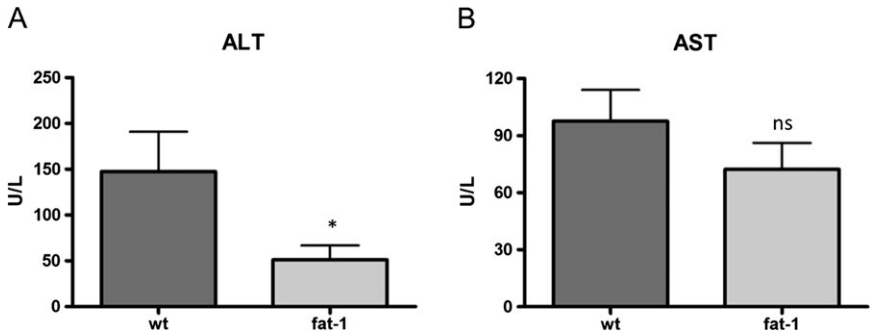

Fig. 5. Assessment of liver damage. DEN-treated fat-1 mice had lower levels of plasma transaminases that wt animals with DEN-induces tumors, indicating less severe liver cell damage in the fat-1 mice, graphs are shown for alanine transaminase (**A**) and aspartate transaminase (**B**) (ns, not significant, $^{*}P < 0.05$).

Table I. PUFA profiles of livers from DEN-treated wt and fat-1 mice (mean ± standard error of the mean) showing higher levels of the n-3 PUFA EPA and DHA in fat-1 liver tissue

PUFA	wt ($n = 6$)	Fat-1 ($n = 9$)	P
n-6 (%)			
AA (20:4 n-6)	9.13 ± 1.20	8.52 ± 0.81	ns
n-3 (%)			
EPA (20:5 n-3)	0.00 ± 0.00	0.17 ± 0.02	<0.0001
DHA (22:6 n-3)	1.01 ± 0.26	4.15 ± 0.46	<0.001
Total	1.01	4.32	
AA/(EPA + DHA)	9.06	1.97	

ns, not significant.

Discussion

The results of this study demonstrate significantly decreased hepatic tumorigenesis in fat-1 mice with endogenously increased tissue n-3 PUFA levels. This was associated with decreased inflammation/regeneration and fibrosis markers such as TNF-α, IL-1β, COX-2, HGF and intrahepatic macrophages as well as decreased activated hepatic stellate cells and myofibroblasts. These data confirm previous observations in the D-GalN/LPS model of acute hepatitis (8) and are consistent with other findings showing that mice fed with DHA-enriched diets had a significant decrease in hepatic COX-2 mRNA expression and inflammatory response (9). Given that TNF-α plays an important role in liver tumorigenesis and DEN-induced carcinogenesis, the decreased levels of TNF-α observed in the fat-1 mice in this study may be an important mechanism underlying the decreased hepatic tumorigenesis.

Several studies have examined the role of fish oil fatty acids in rat models of hepatic carcinogenesis as well as in the fat-1 mouse model. A study with non-7,12-dimethylbenzanthracene-induced liver tumors in rats showed that a diet rich in fish oil leads to a decrease of PGE_2 concentrations in livers and liver tumors. However, there was no decreased tumor incidence as compared with an evening primrose oil-treated group (19). Other studies found decreased formation of hepatic neoplastic foci in fish oil-treated rats with DEN-induced hepatocarcinogenesis (20,21). A recent study showed that n-3 PUFA inhibited HCC cell growth through blocking β-catenin and COX-2 and reduced tumor formation of inoculated hepatoma cells in fat-1

Downloaded from https://academic.oup.com/carcin/article/32/6/897/2463601 by guest on 20 August 2022

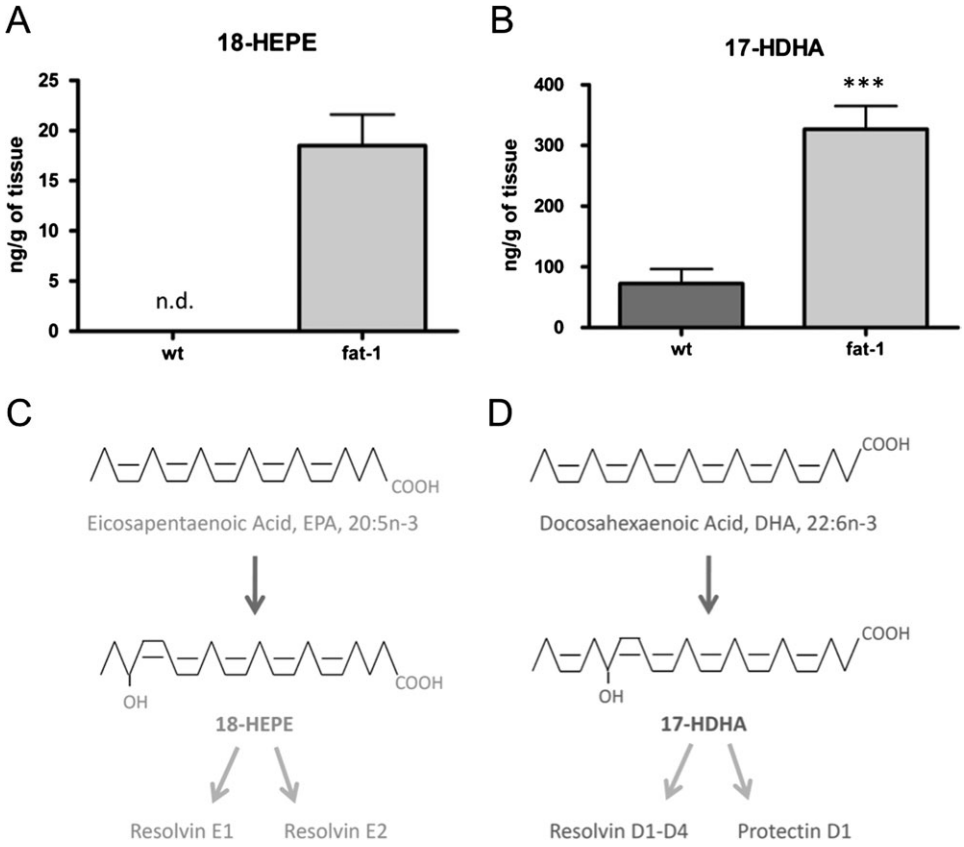

Fig. 6. Formation of 18-HEPE from EPA (**A** and **C**) and of 17-HDHA from DHA (**B** and **D**) is increased in liver tissue from fat-1 mice with DEN-induced tumors as compared to DEN-treated wt animals. 18-HEPE and 17-HDHA could contribute to an anti-inflammatory effect themselves and also be further metabolized to anti-inflammatory resolvins and protectins as shown in (C) and (D) ($^{***}P < 0.001$).

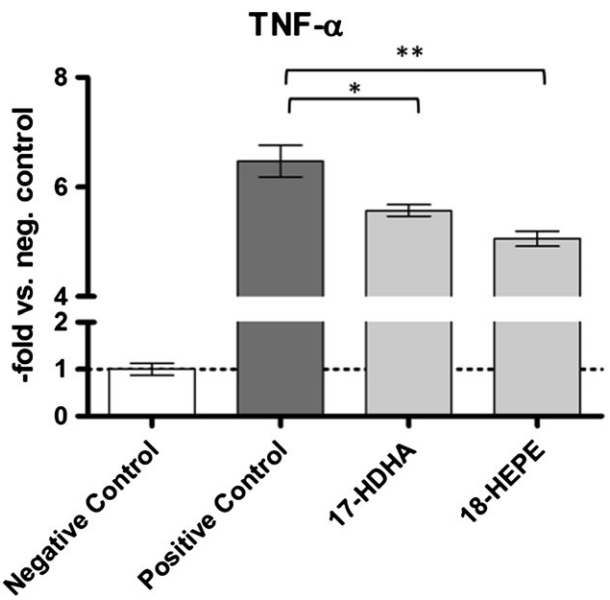

Fig. 7. The n-3 PUFA metabolites 18-HEPE and 17-HDHA at a concentration of 0.5 μM significantly decreased LPS-induced TNF-α secretion from RAW 264.7 murine macrophages ($n = 4$ independent experiments, $^{*}P < 0.05$, $^{**}P < 0.01$).

mice (15), whereas another study with a transgenic liver tumorigenesis approach demonstrated a lower tumor incidence in triple-mutant c-myc/transforming growth factor-alpha/fat-1 mice with a significant decrease of nuclear factor-kappaB protein levels in the fat-1 group and alterations in gene expression patterns. The results presented here confirm this antitumor effect of the increased n-3 PUFA tissue status in fat-1 mice in a chemically induced liver tumorigenesis model.

The results presented here demonstrate significantly higher levels of the EPA metabolite 18-HEPE and the DHA metabolite 17-HDHA in the livers of fat-1 mice with DEN-induced tumors (Figure 6A–D). While the possibility of auto-oxidation processes leading to the increased 18-HEPE and 17-HDHA levels cannot be excluded, it is regardless of the metabolic pathway leading to their formation that these compounds might contribute a significant biological effect by decreasing TNF-α secretion from macrophages. 18-HEPE and 17-HDHA could thereby dampen the inflammatory and regeneratory stimulus and thus, inflammation triggered tumorigenesis in the livers of fat-1 mice. 17-HDHA has been described as an anti-inflammatory compound in the context of experimental liver inflammation previously (9). This was confirmed here. What is more, the data presented here extend this approach to another n-3 PUFA-derived lipid metabolite, the EPA metabolite 18-HEPE.

As 18-HEPE and 17-HDHA are the precursors of protectins and resolvins, which have been reported to be potent anti-inflammatory lipid mediators (22), it is also possible that increased levels of 18-HEPE/17-HDHA contribute to anti-inflammatory effects through their conversion to protectins and resolvins. Another possibility is that the increased levels of 17-HDHA in the livers of DEN-treated fat-1 mice could be an indicator of increased formation of the instable intermediate peroxy-metabolite 17-HpDHA, which was shown to be directly cytotoxic to fast-growing tumor cells (23), an effect that might contribute to an antitumor effect beyond the described mechanism of lowering the TNF-α levels.

This study has some limitations as due to the focus on the biochemical analysis of liver tissue systematic histological workups of

Downloaded from https://academic.oup.com/carcin/article/32/6/897/2463601 by guest on 20 August 2022

whole mouse livers to differentiate between malignant and benign tumors were not done. A direct histological assessment of size and number of lesions in serial sections was not performed. Furthermore, due to low tumor load in DEN-treated fat-1 animals, comparative measurements from isolated tumor tissue were not performed. Regardless of these limitations, the results presented here give strong additional evidence for the formation of protective lipid mediators from n-3 PUFA in the context of liver injury and are, to our knowledge, the first evidence to expand a potential role of these compounds into the context of the inflammation–tumorigenesis pathway in hepatotumorigenesis.

The lipidomics data by Puri *et al.* (11) in non-alcoholic fatty liver disease demonstrate an increased n-6/n-3 free fatty acid ratio in NASH liver tissue as well as stepwise increases in lipoxygenase metabolites such as 15-HETE in plasma samples from patients with non-alcoholic fatty liver disease toward NASH (10). In light of the data presented here, further work will now be necessary to delineate changes in lipid mediator formation in the context of liver pathologies in different stages and in the context of dietary differences in the uptake of n-3/n-6 fatty acids.

Taken together, this study adds new insight to the protective role of n-3 PUFA in liver disease. The data presented here indicate that n-3 PUFA might suppress liver tumorigenesis due to a significant anti-TNF-α effect that is mediated through their hydroxlated metabolites 18-HEPE and 17-HDHA. This, together with the previous *in vitro* and animal studies provides a strong rationale for the potential application of n-3 PUFA supplementation in the alleviation of chronic liver inflammation and prevention of inflammation-triggered liver tumorigenesis.

Funding

Boehringer Ingelheim Foundation (to L.F.K.); American Cancer Society (RSG-03-140-01-CNE); National Institutes of Health (NIH R01 113605) (both to J.X.K.); German Research Foundation (Deutsche Forschungsgemeinschaft) and an MSD Sharp & Dohme GmbH Oncology Scholarship (both to K.H.W.).

Acknowledgements

We thank Jonathan N.Glickman at the Brigham and Women's Hospital in Boston for his help and advice with the histological analyses.

Conflict of Interest Statement: M.R. is the owner of Lipidomix, an analytical service company in Berlin, Germany. The company performed the lipid mediator measurements contained in the manuscript. In order to prevent bias, MR was blinded to the identity of the samples measured and was not part of the writing of the manuscript.

References

1. El-Serag,H.B. *et al*. (2007) Hepatocellular carcinoma: epidemiology and molecular carcinogenesis. *Gastroenterology*, **132**, 2557–2576.
2. El-Serag,H.B. *et al*. (2008) Diagnosis and treatment of hepatocellular carcinoma. *Gastroenterology*, **134**, 1752–1763.
3. Pikarsky,E. *et al*. (2004) NF-kappaB functions as a tumour promoter in inflammation-associated cancer. *Nature*, **431**, 461–466.
4. Sakurai,T. *et al*. (2006) Inaugural article: loss of hepatic NF-{kappa}B activity enhances chemical hepatocarcinogenesis through sustained c-Jun N-terminal kinase 1 activation. *Proc. Natl Acad. Sci. USA*, **103**, 10544–10551.
5. Maeda,S. *et al*. (2005) IKKbeta couples hepatocyte death to cytokine-driven compensatory proliferation that promotes chemical hepatocarcinogenesis. *Cell*, **121**, 977–990.
6. Luedde,T. *et al*. (2007) Deletion of NEMO/IKKgamma in liver parenchymal cells causes steatohepatitis and hepatocellular carcinoma. *Cancer Cell*, **11**, 119–132.
7. Weylandt,K.H. *et al*. (2005) Rethinking lipid mediators. *Lancet*, **366**, 618–620.
8. Schmocker,C. *et al*. (2007) Omega-3 fatty acids alleviate chemically induced acute hepatitis by suppression of cytokines. *Hepatology*, **45**, 864–869.
9. Gonzalez-Periz,A. *et al*. (2006) Docosahexaenoic acid (DHA) blunts liver injury by conversion to protective lipid mediators: protectin D1 and 17S-hydroxy-DHA. *FASEB J.*, **20**, 2537–2539.
10. Puri,P. *et al*. (2009) The plasma lipidomic signature of nonalcoholic steatohepatitis. *Hepatology*, **50**, 1827–1838.
11. Puri,P. *et al*. (2007) A lipidomic analysis of nonalcoholic fatty liver disease. *Hepatology*, **46**, 1081–1090.
12. Kang,J.X. *et al*. (2004) Transgenic mice: fat-1 mice convert n-6 to n-3 fatty acids. *Nature*, **427**, 504.
13. Kang,J.X. (2007) Fat-1 transgenic mice: a new model for omega-3 research. *Prostaglandins Leukot. Essent. Fatty Acids*, **77**, 263–267.
14. Griffitts,J. *et al*. (2010) Non-mammalian fat-1 gene prevents neoplasia when introduced to a mouse hepatocarcinogenesis model omega-3 fatty acids prevent liver neoplasia. *Biochim. Biophys. Acta*, **1801**, 1133–1144.
15. Lim,K. *et al*. (2009) Omega-3 polyunsaturated fatty acids inhibit hepatocellular carcinoma cell growth through blocking beta-catenin and cyclooxygenase-2. *Mol. Cancer Ther.*, **8**, 3046–3055.
16. Ishak,K. *et al*. (1995) Histological grading and staging of chronic hepatitis. *J. Hepatol.*, **22**, 696–699.
17. Knodell,R.G. *et al*. (1981) Formulation and application of a numerical scoring system for assessing histological activity in asymptomatic chronic active hepatitis. *Hepatology*, **1**, 431–435.
18. Rivera,J. *et al*. (2004) Measurement of 20-hydroxyeicosatetraenoic acid in human urine by gas chromatography-mass spectrometry. *Clin. Chem.*, **50**, 224–226.
19. Jelinska,M. *et al*. (2003) Effects of dietary linseed, evening primrose or fish oils on fatty acid and prostaglandin E2 contents in the rat livers and 7,12-dimethylbenz[a]anthracene-induced tumours. *Biochim. Biophys. Acta*, **1637**, 193–199.
20. Kim,Y. *et al*. (2000) Modulation of liver microsomal monooxygenase system by dietary n-6/n-3 ratios in rat hepatocarcinogenesis. *Nutr. Cancer*, **37**, 65–72.
21. Lii,C.K. *et al*. (2000) Suppression of altered hepatic foci development by a high fish oil diet compared with a high corn oil diet in rats. *Nutr. Cancer*, **38**, 50–59.
22. Serhan,C.N. *et al*. (2008) Endogenous pro-resolving and anti-inflammatory lipid mediators: a new pharmacologic genus. *Br. J. Pharmacol.*, **153** (suppl. 1), S200–S215.
23. Gleissman,H. *et al*. (2009) Docosahexaenoic acid metabolome in neural tumors: identification of cytotoxic intermediates. *FASEB J.*, **24**, 906–915.

Received October 29, 2010; revised February 25, 2011; accepted March 5, 2011

Downloaded from https://academic.oup.com/carcin/article/32/6/897/2463601 by guest on 20 August 2022